SCIENTIFIC MINING JOURNAL

The Publication of the Chamber of Mining Engineers of Türkiye

www.mining.org.tr

Original Research

Study on Floor Instability Law of Cemented Filling Mining above a Confined Aquifer

Jiaqi Wang [a,b*],

[a] School of Mines, China University of Mining and Technology, Xuzhou 221116, China
[a] State Key Laboratory of Coal Resources and Safe Mining, China University of Mining and Technology, Xuzhou, Jiangsu, 221116, China

Received: 22 February 2022 • Accepted: 25 July 2023

A B S T R A C T

To solve the problem of floor water inrush in the process of coal mining on a confined aquifer and study the law of floor instability, a cemented filling mining method is proposed in the paper. Using river sand and cement as filling materials, the cementitious material with a concentration of 75% and cement content of 15% has the best flow and mechanical properties. Based on the elastic half-space theory and the bearing characteristics of the backfill, the mechanical model of floor stability is established, the critical criterion of floor instability is proposed, and the relationship between the failure depth of the floor and the location and pressure of the confined aquifer is obtained. The numerical simulation test scheme is designed, and the FLAC3D fluid-structure coupling element is used to explore the instability characteristics of the floor in the mining process. The research results show that the failure depth of the floor will gradually decrease with the increase of the strength of filling materials, the increase of aquifer distance, and the decrease of water pressure. The research results provide a useful reference for the study of the safe mining of coal resources in a confined aquifer.

Keywords: *Confined aquifer, Cementitious materials, Filling mining, Floor, Numerical simulation test.*

Introduction

According to the State Statistics Bureau, China's total energy consumption in 2021 was 4.49×10^9 t of standard coal, of which coal consumption accounts for 60.4% of the total energy consumption (Shen and Wang, 2023). Under such a large mining intensity, most mines have entered the deep level. Especially in the northern mines, they are seriously affected by the extremely thick Ordovician limestone aquifer at the bottom and are very prone to water inrush disasters. According to statistics, from 2015 to 2020, 133 water inrush disasters occurred on the coal seam floor of the northern mine (Yu et al., 2021). At present, China mainly uses drainage and depressurization method, curtain grouting methods, short-face mining methods, strip mining methods, double-face mining methods, segmented retreating mining methods, and filling mining methods to solve the water inrush of coal seam on confined water layer (Han et al. 2021; Sillitoe and Brogi, 2021; Yin et al., 2021). Among them, the drainage and depressurization method can't reduce the Ordovician limestone water with strong water abundance and sufficient supply; The production capacity of short face mining method is low, and the recovery rate of strip mining is low; The layout of the production system of the double face mining is complex; The preparation time of segmented retreating mining method is long; Filling mining method can not only reduce the failure height of overburden but also reduce the failure depth of underlying strata. It is the safest and most reliable measure for mining on a confined aquifer.

Many scholars have done a lot of research on the methods of filling mining to prevent water inrush disasters. For example, Peng (Peng et al., 2021) used the high water material filling method to replace the strip coal pillar on the confined aquifer, analyzed the influence of filling body stability and floor failure, and finally verified the theoretical feasibility of this technology; Du (Du et al., 2021) analyzed the failure law and evolution characteristics of paste filled floor, and predicted the failure range and water inrush of the floor after mining Jia (Jia et al., 2021) quantitatively analyzed the control effect of strip filling replacement mining on surrounding rock deformation of working face and water diversion of the aquifer and Zhang (Zhang et al., 2021) used the methods of similarity simulation, theoretical research, and field practice to study the relationship between support and surrounding rock, ground pressure law of filling face and floor failure law under the condition of gangue filling mining.

* Corresponding author:13852037975@163.com • https://orcid.org/0000-0001-5679-0740

https://doi.org/10.30797/madencilik.1077583

The above research results have promoted the development of mining methods and theories on a confined aquifer, but its application effect is not obvious due to many factors such as filling material production cost, mining efficiency, and ecological protection. Therefore, taking the mining on the confined aquifer of the Zhaoguan energy mine as the background, this paper puts forward the cemented filling mining method to solve the above problems. The cementitious material composed of river sand and cement is designed, the optimal ratio of materials is studied, and the principle of water inrush from the mining floor on a confined aquifer is explained based on theoretical calculation. The numerical simulation test scheme is designed to explore the characteristics of floor instability in the mining process, and the influence law of cementitious material and aquifer distance on floor stability is obtained. The research results provide a useful reference for the study of the safe mining of coal resources on a confined aquifer and further enrich the rock stratum control theory of filling mining.

1. Test conditions

1.1. Geological conditions

Zhaoguan energy mine belongs to Qihe County, De Zhou City, Shandong Province. The minefield is located on the west edge of Dongtai Anticline of Taishan mountain in north China. The overall structural form is a monoclinic structure trending northeast and tending northwest, and the dip angle is generally 5~8°. Zhaoguan energy mine has a total area of 59.2 km^2, a design production capacity of 0.9 mt/a and a service life of 42.8 a. There are 8 minable coal seams in the mine. At present, 11 coal seams are designed to be mined. This coal seam is located above the elevation of –400 m, and the coal thickness is 0.25~2.92 m, with an average of 2 m. The density is 1.5 (g/cm^3) and the minability coefficient is 0.8, which is a stable coal seam. The roof of coal seam 11 is quartzite, with an average thickness of 4 m, compressive strength of 104.2 MPa, and high rock integrity. It belongs to class IV's extremely stable floor. The floor is mudstone with compressive strength of 19.2 MPa, belonging to class I unstable bottom plate. In addition, there is Ordovician limestone 40 m below coal seam 11, which is dense and hard, with karst fractures developed, and the water pressure is about 4.5 MPa. Zhaoguan energy mine adopts cemented filling coal mining method to recover coal. The layout of the first mining face, production system, and rock stratum histogram is shown in Figure 1.

1.2. Mining conditions

The cemented filling coal mining technology designed in this project is based on the production of traditional longwall coal mining methods and uses the fully mechanized excavator to excavate the connecting roadway between the upper and lower roadway of the working face for coal mining. When one connecting roadway passes through the two roadways, the cemented filling material is used for filling, and the other connecting roadway is excavated at the same time. To increase production, multiple excavation faces are often arranged in the working face for mining. Compared with the traditional cemented filling face layout, this technology can realize the simultaneous operation of mining and filling, and reduce the length of the filling pipeline in goaf. It has the advantages of a simple system and high efficiency.

The specific mining process is divided into three stages: excavation of connecting roadway, coal transportation by belt conveyor, and connecting roadway filling. When a connecting roadway is excavated by the fully mechanized excavator, it will immediately be filled with cemented filling materials. Each connecting roadway shall be filled three times to ensure complete filling in the connecting roadway and reduce the lateral pressure on the filling retaining wall at the side of the lower roadway. To ensure that adjacent roadways will not be affected by mining, the two excavation faces shall be separated by more than three connecting roadways (Fahimifar and Zareifard, 2009; Liu et al., 2021; Guo et al., 2021), which is conducive to improving the stability of roof and floor during an unfilled period and reducing the risk of water inrush disaster. The cemented filling mining process is shown in Figure 2.

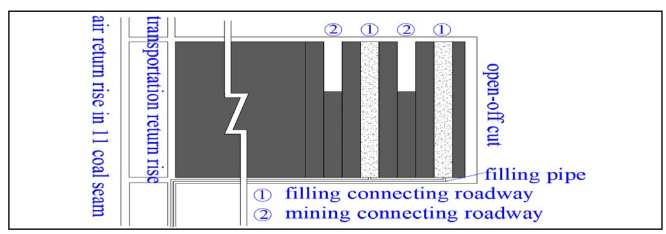

(a) mining and filling technology

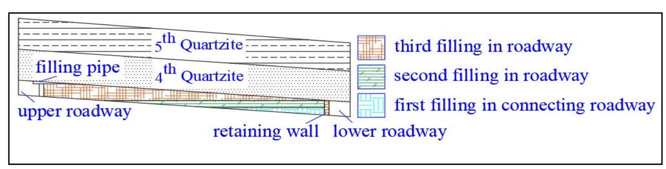

(b) filling technology of each connecting roadway

Figure 2. *Cemented filling coal mining process*

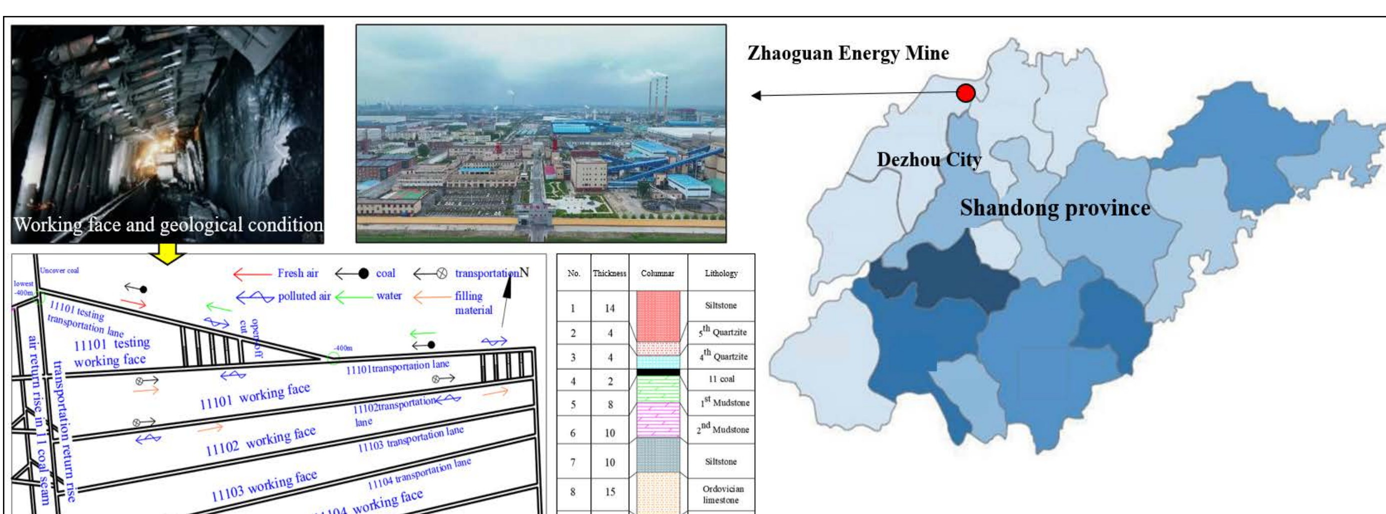

Figure 1. *Working face layout, production system, and rock stratum histogram*

2. Test material

The test material is river sand as aggregate and cement as a binder, which has the characteristics of convenient material acquisition and transportation. The main characteristics of cementitious materials are flow characteristics and mechanical properties. Among them, the mechanical properties are closely related to the stability of the working face floor, which needs to be studied. Six groups of proportioning were designed to study the flow characteristics and mechanical properties. The test scheme is shown in Table 1.

***Table 1**. Test scheme*

Matching number	River sand/%	Cement/%	Concentration /%
S1	90	10	76
S2	90	10	75
S3	90	10	74
S4	90	10	73
S5	85	15	74
S6	95	5	74

2.1. Flow characteristic

The slump is used to describe the flow characteristics of cementitious materials, and the slump of cementitious materials with different ratios is obtained, as shown in Table 2. It can be seen from Table 2 that as the slurry concentration gradually decreases from 76%, the slump of the filling material first increases to the maximum value of 147mm, and then gradually falls. The slump value is the maximum when the slurry concentration is 75%. With the increase of the cement content, the slump of the filling material increases first and then tends to be stable, because the peaceability of the filling material is increased after the cement hydration reaction, increasing the slump. When the cement content reaches 10%, the influence of its content on the slump gradually decreases and the slump tends to be stable.

***Table 2.** Slump test results*

Matching number	River sand/%	Cement/%	Concentration/%	Slump/mm
S1	90	10	76	131
S2	90	10	75	147
S3	90	10	74	128
S4	90	10	72	117
S5	85	15	75	138
S6	95	5	75	96

2.2. Mechanical properties

The cemented filling material is pumped to the goaf to maintain the good stability of the surrounding rock. A reasonable ratio can prevent the destruction of the floor, produce water inrush and support the roof. The filling materials of six schemes are made into standard samples, cured for 28 d, and tested for the stress-strain curves. The samples and test curves are shown in Figure 3 and Figure 4. It can be seen from Figure 4 that the strength of cementitious material from high to low is S6 < S2 < S4 < S1 < S3 < S5, which are 0.55 MPa, 1.22 MPa, 1.24 MPa, 1.42 MPa, 1.49 MPa, and 2.02 MPa respectively. Cementitious materials with a concentration of 75% and a cement content of 15% shall be chosen.

***Figure 3.** Filling material*

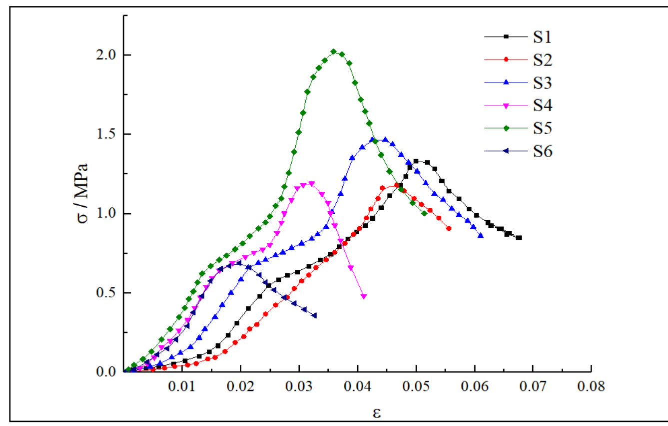

***Figure 4.** Stress-strain curve of filling material sample*

3. Test principle

A mechanical model is established to study the water inrush principle of the floor on the confined aquifer. According to the literature (Batista Rodriguez et al., 2021; Wang et al. 2021; Xu et al., 2021), after mining, the floor rock near the end of the working face and the inner side of the goaf is greatly affected by the shear failure, and water inrush is very easy to occur in these places. Therefore, the filling mining model is established along the advancing direction of the longwall face, as shown in Figure 5. Analyze the stability of the floor (Fu and Wang., 2021; Wu et al., 2021; Ning et al., 2021), in the figure, L_2 is the influence range of coal wall support stress in front of the longwall working face, L_1 is the total width of the filling connecting roadway behind the solid coal, l_a is the width of the connecting roadway, and q_0 is the vertical load that the filling body can bear (taken as 2.18 MPa), γh is the overburden load, k is the stress concentration factor of the front coal wall, P is the pressure of the confined aquifer, and its distance from the coal seam floor is h_0.

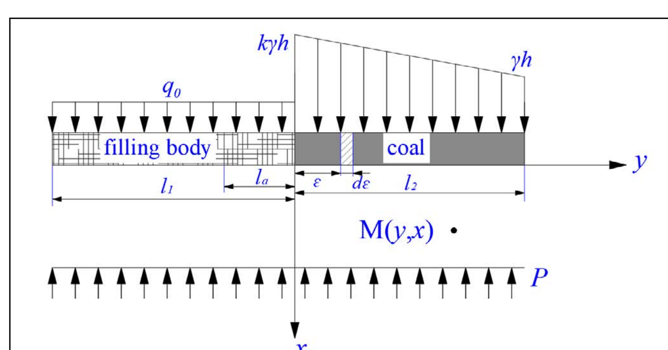

***Figure 5.** Depth failure model of floor*

Then the model roof stress function is:

$$q(\varepsilon)=\begin{cases} q_0 & \varepsilon\in[0,l_1) \\ -\gamma h(\dfrac{1-k}{l_2}\varepsilon+k) & \varepsilon\in[l_1,l_2) \end{cases} \tag{1}$$

The rock strata below the coal seam floor are regarded as isotropic and homogeneous linear deformation bodies. According to the elastic half-space theory (Li et al., 2021; Nam and Bobet, 2006; Ma et al., 2021), the stress state in the floor rock stratum belongs to the plane strain problem, by taking the differential line segment $d\varepsilon$, the additional stress generated by the roof stress on any point M (x, y) of the floor is calculated as follows:

$$\begin{cases} d\sigma_x=\dfrac{2qd_\varepsilon}{\pi}\dfrac{x^3}{\left[x^2+(y-\varepsilon)^2\right]^2} \\ d\sigma_y=\dfrac{2qd_\varepsilon}{\pi}\dfrac{x(y-\varepsilon)^2}{\left[x^2+(y-\varepsilon)^2\right]^2} \\ d\tau_{xy}=\dfrac{2qd_\varepsilon}{\pi}\dfrac{x^2(y-\varepsilon)}{\left[x^2+(y-\varepsilon)^2\right]^2} \end{cases} \tag{2}$$

The stress component function at any point of the floor obtained by integration is:

$$\begin{cases} \sigma_x=\dfrac{2}{\pi}\left(\displaystyle\int_{-l_1}^{0}\frac{-q_0x^3d\varepsilon}{\left[x^2+(y-\varepsilon)^2\right]^2}+\int_0^{l_2}-\gamma h\left[\frac{(1-k)}{l_2}\varepsilon+k\right]\cdot\right. \\ \left.\dfrac{x^3d\varepsilon}{\left[x^2+(y-\varepsilon)^2\right]^2}-\displaystyle\int_{-l_1}^{l_2}\frac{P(h_0-x)^3d\varepsilon}{\left[(h_0-x)^2+(y-\varepsilon)^2\right]^2}\right) \\ \sigma_y=\dfrac{2}{\pi}\left(\displaystyle\int_{-l_1}^{0}\frac{-q_0x(y-\varepsilon)^2d\varepsilon}{\left[x^2+(y-\varepsilon)^2\right]^2}+\int_0^{l_2}-\gamma h\left[\frac{(1-k)}{l_2}\varepsilon+k\right]\cdot\right. \\ \left.\dfrac{x(y-\varepsilon)^2d\varepsilon}{\left[x^2+(y-\varepsilon)^2\right]^2}-\displaystyle\int_{-l_1}^{l_2}\frac{P(h_0-x)(y-\varepsilon)^2d\varepsilon}{\left[(h_0-x)^2+(y-\varepsilon)^2\right]^2}\right) \\ \tau_{xy}=\dfrac{2}{\pi}\left(\displaystyle\int_{-l_1}^{0}\frac{-q_0x^2(y-\varepsilon)d\varepsilon}{\left[x^2+(y-\varepsilon)^2\right]^2}+\int_0^{l_2}-\gamma h\left[\frac{(1-k)}{l_2}\varepsilon+k\right]\cdot\right. \\ \left.\dfrac{x^2(y-\varepsilon)d\varepsilon}{\left[x^2+(y-\varepsilon)^2\right]^2}-\displaystyle\int_{-l_1}^{l_2}\frac{P(h_0-x)^2(y-\varepsilon)d\varepsilon}{\left[(h_0-x)^2+(y-\varepsilon)^2\right]^2}\right) \end{cases} \tag{3}$$

Using Coulomb Moore criterion, the maximum shear stress at any point under the floor can be obtained as follows:

$$\tau_{max}=\sqrt{\tau_{xy}^2+\frac{(\sigma_x-\sigma_y)^2}{2}} \tag{4}$$

It can be seen that when the stress at any point of the floor reaches or exceeds its strength, the point will yield failure. The failure criterion of any point below the floor is established as follows:

$$(\frac{\sigma_x+\sigma_y}{2}\tan\varphi+c)/\sqrt{\tan^2\varphi+1}\geq\tau_{max} \tag{5}$$

Then the instability judgment function of filling coal mining floor is:

$$F(x,y)=(\frac{\sigma_x-\sigma_y}{2}\tan\varphi+c)/\sqrt{\tan^2\varphi+1}-\tau_{max} \tag{6}$$

When f (x, y) < 0, the lower point of the floor is in a yield failure state. Bring the mechanical parameters of Zhaoguan energy mine rock into Equation (6), and take the friction angle in the floor φ = 30 °, cohesion c = 2.8 MPa, the range of influence of support pressure on the front coal body l_2 = 40 m, and stress concentration factor k = 2.1. The critical state curve of floor instability can be made, as shown in Figure 6.

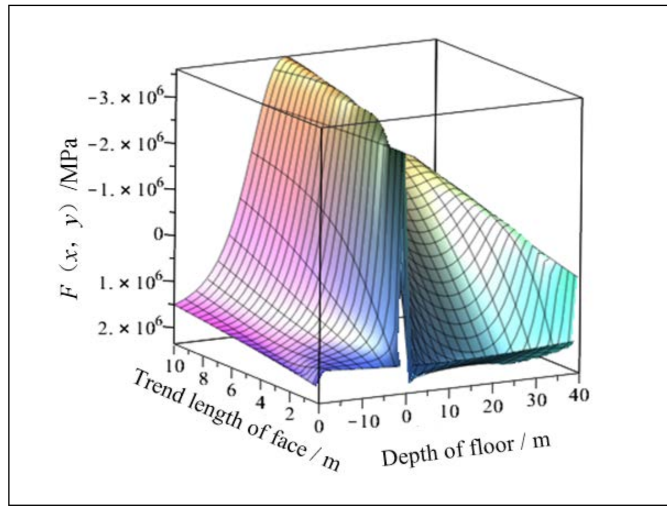

Figure 6. *Distribution of function f (x, y)*

It can be seen from Figure 6 that the maximum failure depth of the coal seam floor is 12.4 m, which occurs 3.49 m behind the solid coal. The maximum depth failure point of the bottom plate is still 37 m away from the confined aquifer. At the same time, the analysis of Equation (6) shows that the strength of the filling body, the location of the confined aquifer, and the water pressure of the aquifer have a great impact on the stability of the floor.

4. Test method and scheme

4.1. Test method

FLAC3D fluid-structure coupling model is used to analyze the law of floor instability under the influence of mining and confined aquifer. In the FLAC3D fluid-structure coupling module, the rock mass is regarded as a porous medium, and the fluid meets Darcy's law and Biot's classical seepage equation (Duan and Zhao, 2021; Zhang et al., 2021; Shi et al., 2021). After entering the fluid-structure coupling calculation mode, the reasonable selection of rock mass and fluid seepage parameters has a great impact on the calculation results. According to the borehole histogram of the Zhaoguan energy mining area and the physical mechanics and seepage parameters of different lithologies in the North China mining area, the numerical simulated coal and rock mass physical mechanics parameters and seepage parameters are designed in Table 3. The mohr-Coulomb constitutive model is adopted for rock mass and fluid is adopted for the fluid_ iso isotropic model.

***Table 3**. The parameters of physical and mechanical coal and rock mass and percolation*

Lithology	Bulk density / $Kg{\cdot}m^{-3}$	tensile strength / MPa	internal friction angle	cohesion / MPa	Elastic model / GPa	Poisson's ratio	Permeability coefficient / $m^2{\cdot}Pa^{-1}{\cdot}sec^{-1}$	Fluid density / $Kg{\cdot}m^{-3}$
Siltstone	2500	0.3	35	3.2	6	3.2	1e-10	1e3
4th Quartzite	2600	0.5	37	3.5	5	2.0	1e-8	1e3
5th Quartzite	2600	0.5	40	8.1	13.9	9.1	1e-8	1e3
11coal	2573	0.08	25	0.5	0.2	0.1	1e-7	1e3
1st Mudstone	2500	0.4	35	2.2	2.25	0.5	1e-10	1e3
2nd Mudstone	2520	0.4	35	2.2	2.25	0.5	1e-10	1e3
Siltstone	2500	0.3	37	3.2	6	3.2	1e-9	1e3
Ordovician limestone	2610	0.3	35	3.6	3.3	2.0	1e-8	1e3

The numerical calculation model of cemented filling mining is established, and the size of the model is 100x120x67 m. Fully constrained boundary conditions are adopted at the bottom and around the model, vertical stress of 7.5 MPa is applied at the top to simulate the pressure of overburden on the model and a permeable seepage boundary with a fixed water pressure of 4.5 MPa is applied at the bottom to simulate the pressure of confined aquifer. After excavation, the goaf adopts drainage boundary conditions (Ma et al., 2019; Ma et al., 2019; Ma et al., 2021), and the model is established as shown in Figure 7. ① ~ ④ in the Figure 7 is the first step of filling and mining to the fourth step of filling and mining. The width of each connecting roadway is 4.5 m.

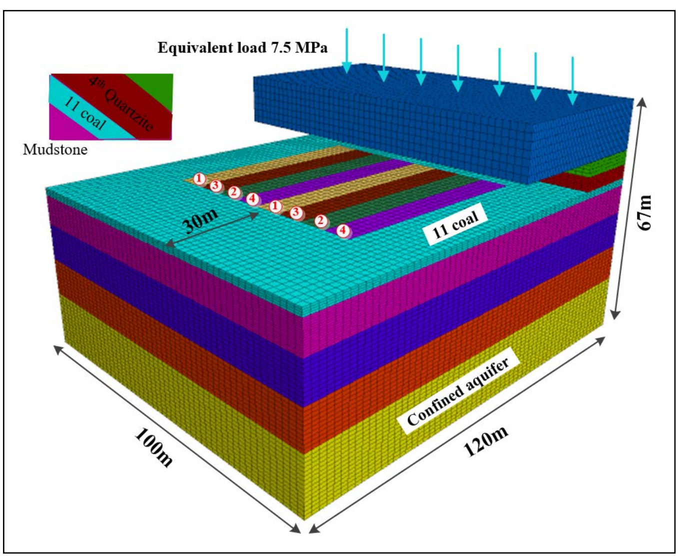

***Figure 7.** Numerical model of cemented filling mining*

4.2. Test scheme

After the model is established, the initial balance calculation is carried out, and then mining and filling are carried out. The design working face adopts two excavation faces for mining, and the overall mining sequence is Mining ① - filling ① - mining ② - filling ② - mining ③ - filling ③ - mining ④. In the mining process of working face, the development of a plastic zone of floor and pore water pressure are observed and analyzed.

In the subsequent tests, three parameters of backfill strength, aquifer distance, and water pressure were adjusted to analyze their influence on the stability of the floor. The strength of the filling body is selected from six proportioning schemes such as S6, S2, S4, S1, S3, and S5. The aquifer distance is designed as 10 m, 20 m, 30 m, 40 m, 50 m, 60 m, 70 m, 80 m, and 90 m. The water pressure of the aquifer is 0 MPa, 0.5 MPa, 1.0 MPa, 1.5 MPa, 2.0 MPa, 2.5 MPa, 3.0 MPa, 3.5 Mpa, 4.0 Mpa, 4.5 MPa and 5 MPa respectively.

5. Test results and discussion

5.1. Law of floor instability during cemented filling mining

During the mining cycle, the state zone module is used to analyze the plastic zone of the excavation and filling area, and the distribution characteristics of the plastic failure zone of the floor are obtained as shown in Figure 8.

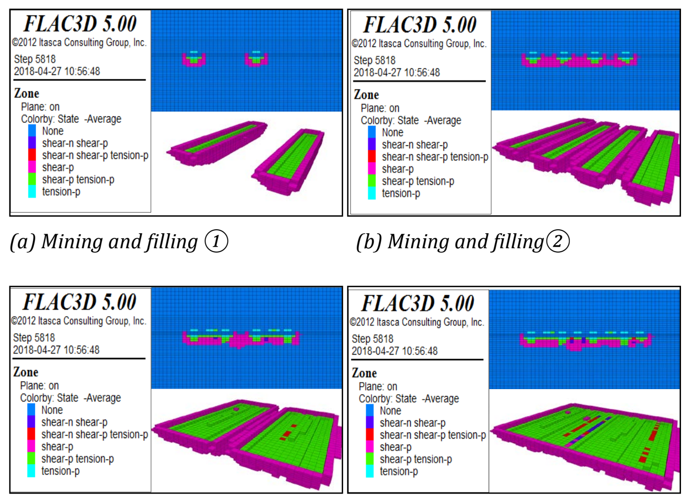

(a) Mining and filling ① *(b) Mining and filling②*

(c) Mining and filling ③ *(d) Mining and filling④*

***Figure 8.** Distribution characteristics of plastic failure of the floor*

It can be seen from Figure 8 that the failure type of rock mass in the process of excavation and filling is mainly shear failure. With the continuous excavation and filling of connecting roadways, the plastic failure area of the floor rock mass in the mining area is continuously connected and deepened. When excavating and filling ①, the maximum failure depth of the plastic area of the coal seam floor is 4 m and symmetrically distributed. When excavating and filling ④, The maximum damage depth of the coal seam floor is 7 m, which occurs in the middle of the mining area and is far away from the Ordovician limestone. The water diversion failure zone cannot relate to the uplift zone of the confined water layer (Yan et al., 2021; Zhang and Wang, 2007; Zhang et al., 2015), which eliminates the risk of water inrush.

At the same time, when a connecting roadway is excavated, the coal near the roadway is vulnerable to shear damage. The "skip mining" method is adopted to mine at a far position from the mined connecting roadway. After the filling body is stable, mining at a closer position can effectively prevent the occurrence of coal wall caving and other phenomena. As the roof lithology of the Zhaoguan energy mine is limestone with good stability, and the above methods are used for coal mining, the roof stability is good. Tension failure occurs only in the middle of the connecting roadway, and the depth is less than 1 m.

4.2.2. Analysis of pore water pressure in mining

In the process of mining, the pore water pressure of the model is analyzed by calling the pore pressure module, and the pore water pressure distribution is shown in Figure 9.

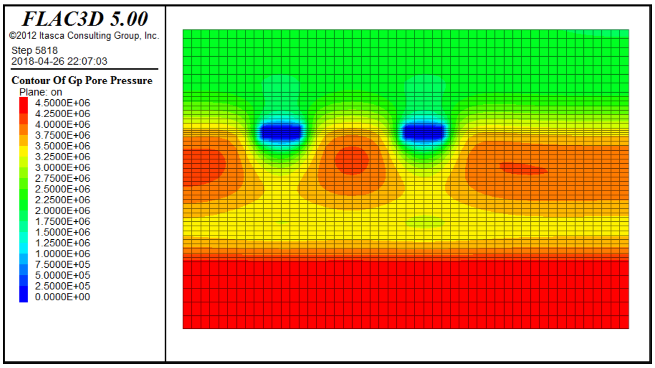

(a) Mining and filling ①

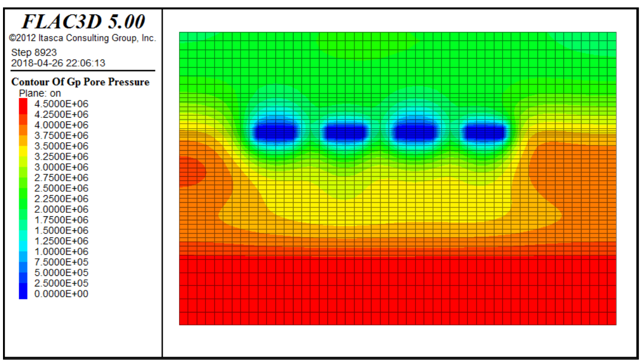

(b) Mining and filling ②

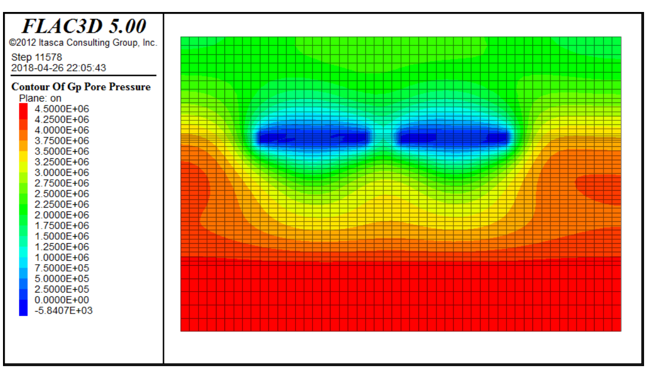

(c) Mining and filling ③

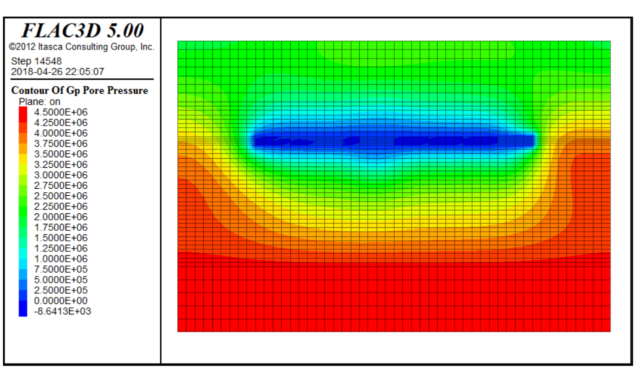

(d) Mining and filling ④

Figure 9. *Pore water pressure distribution*

It can be seen from Figure 9 that the pore water pressure increases fastest on both sides of the connecting roadway and the mining area. It can be seen that water inrush disasters are very easy to occur near the goaf and the mining area boundary, and attention should be paid to the prevention and control of water inrush in this area. In addition, the water-conducting boundary of bedrock (Zhou et al., 2016; Zhang et al., 2015; Yin et al., 2020) always exceeds the mining boundary, and the seepage velocity of the lower rock stratum is always greater than that of the upper rock stratum.

5.2. Law of floor instability under the influence of strength of cementitious material

The influence law of cementitious material on the failure depth of the floor is obtained, as shown in Figure 10. As can be seen from Figure 10, as the strength of the filling body gradually increases, the failure depth of the floor gradually decreases. When the strength of the filling body is 0.55 MPa, 1.22 MPa, 1.24 MPa, 1.42 MPa, 1.49 MPa, and 2.02 MPa, the failure depth of the floor is 14.02 m, 12.89 m, 10.34 m, 9.22 m, 8.89 m, and 8.02 m respectively. Therefore, filling cementitious materials can effectively prevent water inrush.

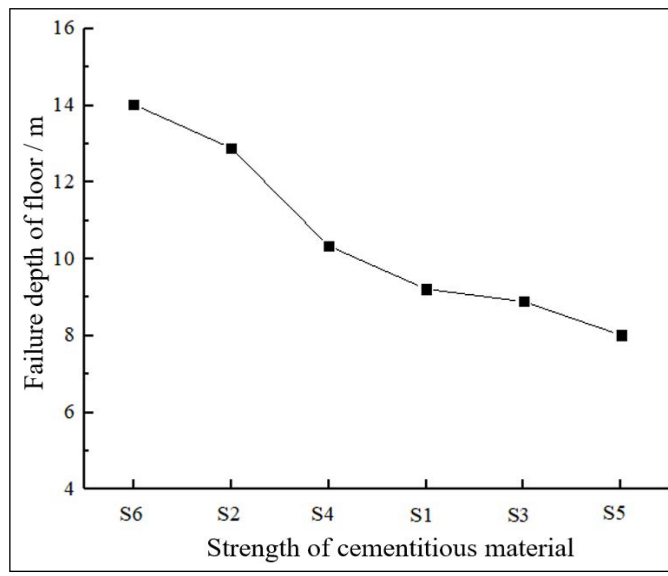

Figure 10. *Effect of the strength of cementitious material on failure depth of the floor*

5.3. Law of floor instability under the influence of aquifer distance and water pressure

The influence law of aquifer distance on floor failure depth is obtained, as shown in Figure 11. The influence law of water pressure on the failure depth of the floor is also obtained, as shown in Figure 12. As can be seen from Figures 11 and 12, with the continuous increase of the pressure of the confined aquifer, the failure depth of the bottom plate gradually increases. When the pressure of the confined aquifer is greater than 2 MPa, the failure depth of the bottom plate increases obviously. With the gradual increase of the distance between the confined aquifer and the coal seam, the damage depth of the floor gradually decreases. However, it can be seen that the floor of the working face is always greatly affected by the confined aquifer when the aquifer depth increases from 10 m to 90 m. It can be seen that the problem of the confined aquifer cannot be ignored in the safe mining of coal mines, and the guarantee measures for the safe mining on the confined aquifer should always be taken.

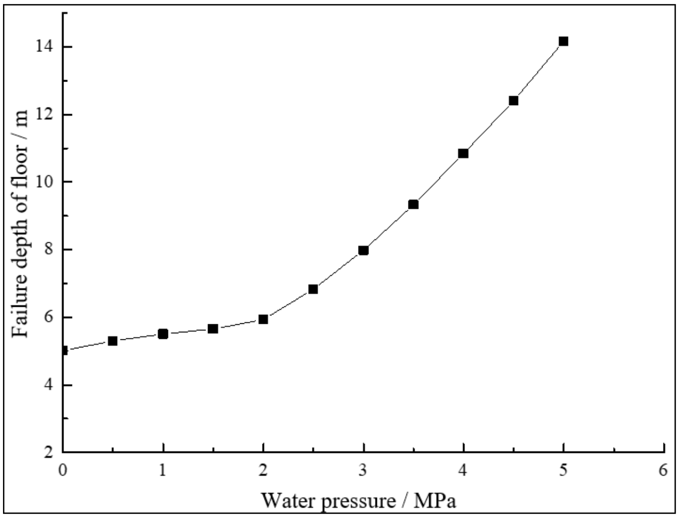

***Figure 11**. Effect of water pressure on failure depth of the floor*

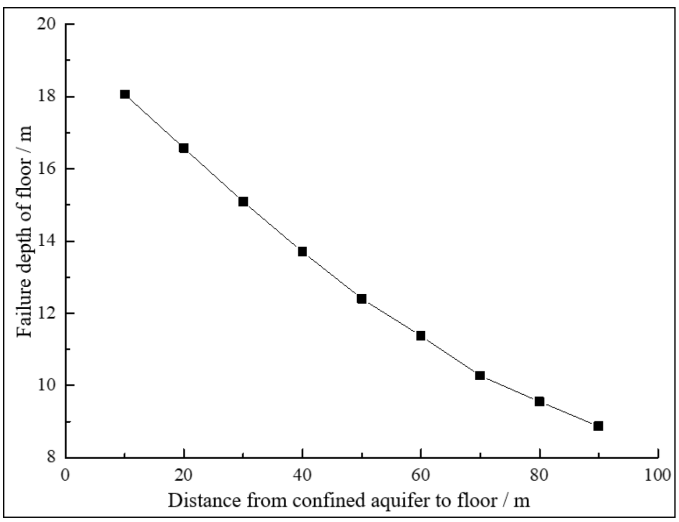

***Fig. 12** Effect of confined aquifer depth on failure depth of the floor*

6. Conclusion

To realize safe mining above the confined aquifer, this paper puts forward the cemented filling mining method, designs the best ratio of cemented materials, and explains the principle of water inrush from the mining floor on the confined aquifer based on theoretical calculation. The numerical simulation test scheme is designed to explore the characteristics of floor instability in the mining process. The specific conclusions are as follows:

(1) Given the technical problems of mining on the confined aquifer in the Zhaoguan energy mine, a cemented filling mining method is proposed. Combined with the actual conditions of the mining area, the filling material ratio of Yellow River Sediment: Cement = 0.85:0.15 is designed, the slump reaches 138 mm and the strength reaches 2.02 MPa.

(2) Based on the elastic space half-space theory, the mechanical model of floor instability in cemented filling coal mining is established, the critical criterion formula of floor instability is deduced, the principle of floor instability on confined aquifer is explained, and the maximum failure depth of working face floor is determined to be 12.4 m. At the same time, it is obtained that the strength of cemented material, aquifer distance, and aquifer water pressure are the main factors affecting floor stability.

(3) Based on the analysis of the calculation results of the fluid-structure coupling numerical model, it can be seen that the surrounding rock damage during the excavation and filling of the connecting roadway is mainly shear damage, and water inrush is very easy to occur in the goaf and the boundary of the mining area. At the same time, with the increase in the strength of cementitious material, the increase in aquifer distance, and the decrease in water pressure, the failure depth of the floor decreases gradually.

(4) The numerical simulation test shows that when the aquifer distance is 40 m, the water pressure is 4.5 MPa and the strength of cementitious material is 2.02 MPa, the failure depth of the floor is far less than 15 m, which is consistent with the theoretical settlement results, which proves that this method can effectively solve the problem of floor water inrush.

Data availability statement

The original contributions presented in the study are included in the article, further inquiries can be directed to the corresponding author.

Author contributions

Jiaqi Wang: Conceptualization, Model investigation, Data curation, Writing - original draft.

Acknowledgments

Thanks to the staff of Zhaoguan energy mine.

Conflicts of interest

The author declare no conflicts of interest.

References

Batista-Rodriguez, J. A., Perez-Flores, M. A., Almaguer-Carmenates, Y., Blanco-Moreno, J. A., Lopez-Saucedo, F. D. J., & Batista-Cruz, R. Y. 2021. Using electrical resistivity tomography to evaluate the relationship between groundwater potential and tectonism in northeast Mexico. Revista Mexicana de Ciencias Geologicas, 38(1), 18-28.

Du, Y., Liu, W., Meng, X., Pang, L., & Han, M. 2021. Effect of Crack Propagation on Mining-Induced Delayer Water Inrush Hazard of Hidden Fault. Geofluids, 2021.

Duan, H., & Zhao, L. 2021. New evaluation and prediction method to determine the risk of water inrush from mining coal seam floor. Environmental Earth Sciences, 80(1), 1-13.

Fu, B., & Wang, B. 2021. An Influence Study of Face Length Effect on Floor Stability under Water-Rock Coupling Action. Geofluids, 2021.

Fahimifar, A., & Zareifard, M. R. 2009. A theoretical solution for analysis of tunnels below groundwater considering the hydraulic–mechanical coupling. Tunnelling and Underground Space Technology, 24(6), 634-646.

Guo, J., Zhang, Q., Li, Q., & Chen, Z. 2021. Study on permeability evolution mechanism of aquifer coal seam roof sandstone under plastic flow. Geomechanics and Geophysics for Geo-Energy and Geo-Resources, 7(3), 1-22.

Han, D., Currell, M. J., & Guo, H. 2021. Controls on distributions of sulphate, fluoride, and salinity in aquitard porewater from the North China Plain: Long-term implications for groundwater quality. Journal of Hydrology, 603, 126828.

Jia, J., Hao, X., Zhao, G., Li, Y., Chuai, X., Huang, L., & Zhan, R. 2021. Evolution analysis of microseismic events before and after mining through large-scale weak zone with high confined water. Advances in Civil Engineering, 2021.

Li, A., Mu, Q., Ma, L., Liu, C., Wang, S., Wang, F., & Mou, L. 2021. Numerical Analysis of the Water-blocking Performance of a Floor with a Composite Structure under Fluid–solid Coupling. Mine Water and the Environment, 40(2), 479-496.

Liu, Z., Dong, S., Wang, H., Wang, X., Nan, S., & Liu, D. 2021. Macroscopic and mesoscopic development characteristics of the top strata of Middle Ordovician limestone in the Hanxing mining area. Environmental Earth Sciences, 80(16), 1-17.

Ma, K., Sun, X. Y., Tang, C. A., Yuan, F. Z., Wang, S. J., & Chen, T. 2021. Floor water inrush analysis based on mechanical failure characters and microseismic monitoring. Tunnelling and Underground Space Technology, 108, 103698.

Ma, D., H Duan, Liu, J., Li, X., & Zhou, Z. 2019. The role of gangue on the mitigation of mining-induced hazards and environmental pollution: an experimental investigation. Science of the Total Environment, 664(MAY 10), 436-448. doi: 10.1016/j.scitotenv.2019.02.059

Ma, D., Duan, H., Li, X., Li, Z., Zhou, Z., & Li, T. 2019. Effects of seepage-induced erosion on nonlinear hydraulic properties of broken red sandstones. Tunnelling and Underground Space Technology, 91(SEP.), 102993. doi: 10.1016/j.tust.2019.102993

Ma, D., Zhang, J., Duan, H., Huang, Y., & Zhou, N. 2021. Reutilization of gangue wastes in underground backfilling mining: overburden aquifer protection. Chemosphere, 264(Pt 1), 128400. doi: 10.1016/j.chemosphere.2020.128400

Ning, S., Zhu, W., Yi, X., & Wang, L. 2021. Evolution Law of Floor Fracture Zone above a Confined Aquifer Using Backfill Replacement Mining Technology. Geofluids, 2021.

Nam, S. W., & Bobet, A. 2006. Liner stresses in deep tunnels below the water table. Tunnelling and Underground Space Technology incorporating Trenchless Technology Research, 21(6), 626-635.

Peng, Z., Chen, L., Hou, X., Ou, Q., Zhang, J., & Chen, Y. 2021. Risk assessment of water inrush under an unconsolidated, confined aquifer: the application of GIS and information value model in the Qidong Coal Mine, China. Earth Science Informatics, 1-14.

Shen, S. M., & Wang, H. Y. 2023. Asymmetric Multifractal Analysis of the Chinese Energy Futures and Energy Stock Markets under the Impact of COVID-19. Fluctuation and Noise Letters, 22(01), 2350002.

Sillitoe, R. H., & Brogi, A. 2021. Geothermal systems in the northern apennines, italy: modern analogues of carlin-style gold deposits. Economic Geology, 116(7), 1491-1501.

Shi, X., Zhou, H., Sun, X., Cao, Z., & Zhao, Q. 2021. Floor damage mechanism with cemented paste backfill mining method. Arabian Journal of Geosciences, 14(2), 1-9.

Wang, Z., Li, W., & Hu, Y. 2021. Experimental study on mechanical behavior, permeability, and damage characteristics of Jurassic sandstone under varying stress paths. Bulletin of Engineering Geology and the Environment, 1-17.

Wu, J., Jing, H., Meng, Q., Yin, Q., & Yu, L. 2021. Assessment of cemented waste rock backfill for recycling gangue and controlling strata: creep experiments and models. Environmental Science and Pollution Research, 1-17.

Xu, C., Lu, C., & Wang, J. 2021. Interval uncertainty analysis of a confined aquifer. Scientific reports, 11(1), 1-5.

Yu, G. F., Yuan, L., & Ren, B. 2021. Big data cloud platform for monitoring and early warning of water disaster from coal floor and its application feasibility in Huaihe Energy Group [J/OL]. Journal of China Coal Society, 08-05.

Yin, H., Xu, B., Yin, S., Tian, W., Yao, H., & Meng, H. 2021. Prevention of Water Inrushes in Deep Coal Mining over the Ordovician Aquifer: A Case Study in the Wutongzhuang Coal Mine of China. Geofluids, 2021.

Yan, H., Zhang, J., Li, B., & Zhu, C. 2021. Crack propagation patterns and factors controlling complex crack network formation in coal bodies during tri-axial supercritical carbon dioxide fracturing. Fuel, 286, 119381. doi: 10.1016/j.fuel.2020.119381

Yin, H., Zhao, C., Zhai, Y., Sang, S., Zhao, H., Li, S., ... & Zhuang, X. 2020. Application of comprehensive support techniques to roadway tunneling in vicinity of Ordovician carbonate confined aquifers under complicated tectonic conditions. Carbonates and Evaporites, 35(4), 1-14.

Zhang, J., Guo, L., Mu, W., Liu, S., & Zhao, D. 2021. Water-inrush Risk through Fault Zones with Multiple Karst Aquifers Underlying the Coal Floor: A Case Study in the Liuzhuang Coal Mine, Southern China. Mine Water and the Environment, 1-11.

Zhang, Y. 2021. Mechanism of Water Inrush of a Deep Mining Floor Based on Coupled Mining Pressure and Confined Pressure. Mine Water and the Environment, 40(2), 366-377.

Zhang, Q. L., & Wang, X. M. 2007. Performance of cemented coal gangue backfill. Journal of Central South University of Technology, 14(2), 216-219. doi: 10.1007/s11771-007-0043-y

Zhang, J., Qiang, Z., Sun, Q., Gao, R., Germain, D., & Abro, S. 2015. Surface subsidence control theory and application to backfill coal mining technology. Environmental Earth Sciences, 74(2), 1439-1448. doi: 10.1007/s12665-015-4133-0

Zhou N, Han X, Zhang J, et al. 2016. Compressive deformation and energy dissipation of crushed coal gangue[J]. Powder Technology, 297:220–228. doi: 10.1016/j.powtec.2016.04.026